

Dynamic Burstein–Moss shift in GaAs and GaAs/AlGaAs multiple quantum well structures

D. J. Erskine, A. J. Taylor, and C. L. Tang

Materials Science Center, Cornell University, Ithaca, New York 14853

(Received 29 May 1984; accepted for publication 19 September 1984)

Time-resolved studies of the dynamic Burstein–Moss shift of the absorption edge following intense photoexcitation are reported for room-temperature samples of GaAs and GaAs/AlGaAs multiple quantum well (MQW) structures. Band-filling times, which correspond to the redistribution of electrons from an energy of 0.5 eV above the bottom of the conduction band to an energy of 0.15 eV, are found to be 1.7 to 1.3 ps for GaAs in the carrier density range of $0.5\text{--}2.0 \times 10^{19} \text{ cm}^{-3}$ and 1 ps for a MQW structure at a density of $2 \times 10^{19} \text{ cm}^{-3}$. An approximate rate equation model is presented which agrees reasonably well with the experimental results.

In this letter we report on a picosecond effect which we observed in GaAs and multiple quantum well (MQW) structures, but not in $\text{Al}_{0.32}\text{Ga}_{0.68}\text{As}$. We believe that this effect is due to the dynamic Burstein–Moss¹ shift of the absorption edge following intense photoexcitation. Very briefly, this effect is related to the relaxation of hot electrons initially photoexcited from the valence band by a 100-fs pulse of 2-eV laser photons into a narrow band of excited states approximately 0.5 eV above the conduction-band minimum. In the case of GaAs, 2-eV photons can induce direct transitions from the heavy hole, light hole, and split-off valence bands. In the case of $\text{Al}_{0.32}\text{Ga}_{0.68}\text{As}$, because of the larger band-gap direct transition from the split-off band is not allowed for 2-eV photons. Following the short pulse excitation, the electrons scatter from the initially photoexcited states by optical phonons into the satellite valleys in a time less than 0.1 ps as previous femtosecond studies showed.² The carriers subsequently scatter back and relax to the bottom of central valley. As the carriers fill up the states near the bottom of the central valley, the corresponding quasi-Fermi level and, hence, the absorption band edge shift to the blue, known as the Burstein–Moss shift. For sufficiently high photoexcited carrier densities, as in our experiment, this shift can lead to saturation of the split-off transition in GaAs. Thus, this saturation effect is a convenient probe of the time it takes for a nonequilibrium distribution high in the conduction band to relax to the bottom of the conduction band. The approximately 1-ps characteristic time we observed reflects this band-filling process. A similar effect has been reported in Ge having an approximately 10-ps characteristic time.³ Although other authors have reported related band-filling effects in GaAs,³ we believe that this is the first measurement of this effect in room-temperature GaAs and MQW structures with femtosecond resolution so that the temporal development of the band-filling process is clearly isolated from the effects of the photoexciting pulse.

The equal-pulse correlation technique² is used to study this band-filling effect. Briefly, two 100-fs, 612-nm pulses from a passively mode-locked ring dye laser operating in the colliding-pulse mode are transmitted through the sample. The pulses are orthogonally polarized, collinearly propagating, and have a delay τ between them. The time-averaged combined transmitted flux of both pulses is measured as a function of τ . The experimental details are described in Ref. 2, except that the dither amplitude in the signal processing

system was increased to improve the signal-to-noise ratio, yielding a resolution of 100 fs.

Three samples were measured: (1) a layer of undoped GaAs 0.3 μm thick clad by 0.15- μm layers of $\text{Al}_{0.6}\text{Ga}_{0.4}\text{As}$; (2) a MQW structure having five 15-nm-thick undoped GaAs well between 70-nm $\text{Al}_{0.6}\text{Ga}_{0.4}\text{As}$ barriers; (3) an uncladded layer of $\text{Al}_{0.32}\text{Ga}_{0.68}\text{As}$ about half an absorption length thick. The substrates were removed in a 375- μm circle by chemical etching.

Scans for GaAs, the MQW, and AlGaAs are shown in Figs. 1 (a), 1 (b), and 1 (c), respectively. The peak centered around $\tau = 0$ is the increase in time-averaged combined transmitted flux of both pulses due to the saturation of the photoexcited states by the pulses.² The relaxation time of carriers out of the photoexcited state can be determined from a comparison of the width of this central peak relative to the autocorrelation of the laser pulse.² Here we consider the rising wings on either side of the central peak, which reveal rise

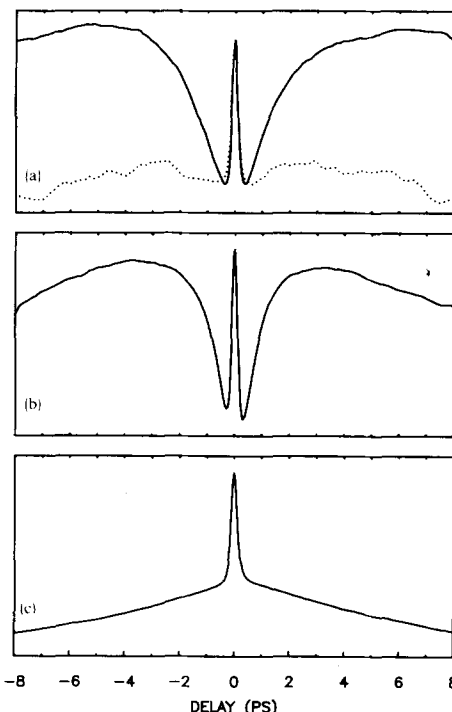


FIG. 1. (a) Experimental scans of transmission vs τ for GaAs at $P = 0.6 \text{ mW}$ (solid line) and $P = 0.2 \text{ mW}$ (dotted line). The wing rise time for the solid curve is $1.6 \pm 0.2 \text{ ps}$. (b) Experimental scan for MQW at $P = 0.6 \text{ mW}$ and with a wing rise time of $1.0 \pm 0.2 \text{ ps}$. (c) Experimental scan for $\text{Al}_{0.32}\text{Ga}_{0.68}\text{As}$ at $P = 0.6 \text{ mW}$.

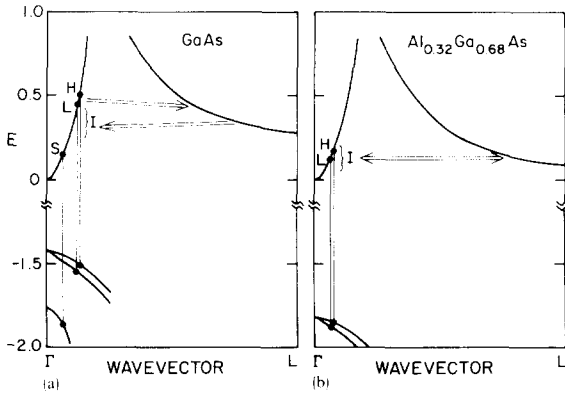


FIG. 2. Schematic band structure of GaAs and $\text{Al}_{0.32}\text{Ga}_{0.68}\text{As}$ between central and L valley. Energy E is in eV. Horizontal dimensions not drawn to scale. H , L , and S indicate the conduction levels optically connected by 2.02-eV photons to the heavy, light, and split-off valence bands. I is the region of central valley levels roughly isoenergetic with the L valley minimum. The arrows suggest the two stages of the band-filling process: initial occupation of the L valley, and subsequent draining through region I .

times of 1.3 to 1.7 ± 0.2 ps for GaAs and 1 ± 0.2 ps for the MQW. The rising wings exhibit a threshold behavior as a function of input power, P (or carrier density n_e) and are seen only for $P > 0.2$ mW (8×10^{-5} J/cm²/pulse or $n_e > 0.4 \times 10^{19}$ cm⁻³) for GaAs and $P > 0.1$ mW ($n_e > 0.3 \times 10^{19}$ cm⁻³) for the MQW structure. The pulse repetition rate is 10^8 /s and spot diameter is $1.8 \mu\text{m}$. The magnitude of the rising wings increases linearly with P up to the highest power studied, $P = 1$ mW, but the characteristic rise time does not depend strongly on P . No rising wings were seen for $\text{Al}_{0.32}\text{Ga}_{0.68}\text{As}$ in the power range studied (0.01–1 mW). For $\tau > 6$ ps for all samples the transmission decreases slowly and monotonically out to at least 22 ps.

We believe the increase in transmission which forms the rising wing in GaAs and the MQW structure is caused by the saturation of photoexcited levels in the conduction band connected to the split-off band transition. Figure 2 (a) displays a schematic of the band structure of GaAs.⁴ There are three distinct transitions for our 2.02-eV photon: from the heavy hole, light hole, and split-off valence bands to conduction-band levels at $E_H = 0.51$ eV, $E_L = 0.45$ eV, and $E_S = 0.15$ eV, respectively. Because of the smaller density of states at energy E_S , the split-off band transition contributes about 15% to the total unsaturated absorption, the remainder being divided roughly equally between the heavy and light hole transitions. Our picture of the relaxation process following photoexcitation is as follows. The bulk of photoexcited electrons is deposited in the Γ valley of the conduction band at H and L . Most of these electrons scatter to the outer valleys due to the much larger number of unoccupied states there. Cooling in all valleys then proceeds via phonon emission. The outer valleys drain through region I [Fig. 2 (a)] in the Γ valley which is isoenergetic with the L valley. The rate of this draining process is controlled by both the L to Γ scattering rate (which is roughly ten times smaller than the Γ to L rate) and the scattering rate out of I due to intravalley polar-optical and carrier-carrier scattering. This process continues until the reservoir of electrons in the outer valleys is depleted. As the outer valleys drain, the bottom of the central valley fills with electrons, which, for large enough n_e ,

can partially saturate the low-lying split-off band transition, thus increasing the transmission of a suitably delayed pulse. The characteristic rise time of the wings then reflects the time it takes the electrons originally deposited with 0.5 eV of energy to establish a distribution at the bottom of the conduction band with significant population at 0.15 eV.

As shown in Fig. 2 (b), the band structure of $\text{Al}_{0.32}\text{Ga}_{0.68}\text{As}$ is different from GaAs in that there is no 2.02-eV transition from the split-off band. Therefore, for AlGaAs samples to exhibit this rising wing, a significant electron population would have to fill the conduction band up to the level of the light hole transition at $E_L = 0.12$ eV, which lies 0.03 eV above the bottom of the L valleys. The total number of states from the bottom of the conduction band up to the light hole transition is 5×10^{19} cm⁻³ in AlGaAs, which is ten times larger than the total number of states up to the split-off transition in GaAs. To achieve this final electron density in AlGaAs, an incident power of 5 mW would be necessary, which is considerably higher than the power range studied. Moreover, since the carrier distribution is being probed at the same place it is being pumped (H and L), there would not be the temporal delay between photoexcitation and the band-filling process which is observed in the rising wing in GaAs. Our band-filling hypothesis is therefore supported by the absence of a rising wing in AlGaAs.

To compare this band-filling picture to our data, we have numerically solved an approximate rate equation model for the central and outer valleys of the conduction band in GaAs. In this model, the n th level consists of all of those states in the Γ or L valleys (the X valley is not considered) with energies E above the bottom of the Γ valley such that $(n-1)\hbar\omega_L < E < n\hbar\omega_L$, where $\hbar\omega_L = 0.036$ eV is the optical phonon frequency in the central valley. To keep the model reasonably simple, we consider only unscreened intravalley polar optical phonon and intervalley phonon scattering. Screening could change the scattering rates, although probably no more than a factor of 2. It is nevertheless ignored because existing theory on screening is valid only for equilibrium carrier distributions. In the present case, the distribution is far from equilibrium. Carrier-carrier scattering, which also depends on the screening parameter, and other

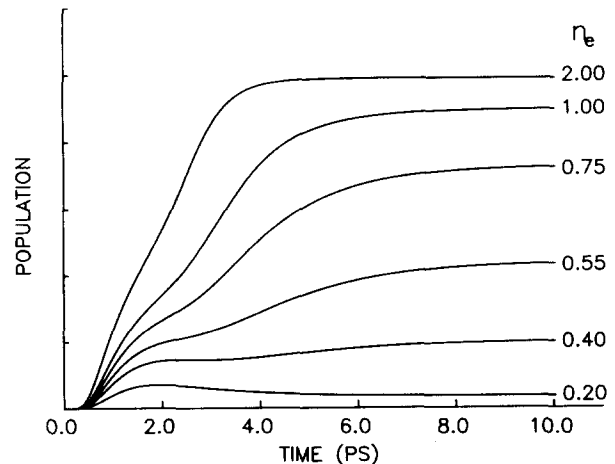


FIG. 3. Calculated time evolution of the electron population at the split-off transition, C_s , for a range of values of n_e (in units of 10^{19} cm⁻³). The units of the vertical axis are arbitrary.

elastic scattering processes clearly play an important role in thermalizing the distribution. However, the rate of cooling is determined mainly by phonon emission, and their inclusion would make the theory too complicated for the present purpose. As a result of all these limitations implicit in the model,

the calculated results should clearly be regarded only as an indication of what is to be expected qualitatively theoretically.

The resultant rate equations for electrons in the n th level of the central valley, C_n , or the L valley, L_n , are

$$\frac{dC_n}{dt} = -C_n \left(\frac{A_n^C(C_{n+1}^0 - C_{n+1})}{C_{n+1}^0} + \frac{E_n^C(C_{n-1}^0 - C_{n-1})}{C_{n-1}^0} + \frac{A_n^{CL}(L_{n+1}^0 - L_{n+1})}{L_{n+1}^0} + \frac{E_n^{CL}(L_{n-1}^0 - L_{n-1})}{L_{n-1}^0} \right) + (C_n^0 - C_n) \frac{[E_{n+1}^C C_{n+1} + A_{n-1}^C C_{n-1} + E_{n+1}^{LC} L_{n+1} + A_{n-1}^{LC} L_{n-1}]}{C_n^0} \quad 1 \leq n \leq 18, \quad (1)$$

where L_n is the electron population of the n th level of the L valley, A_n^C and E_n^C are the polar optical phonon absorption and emission rates for the n th state of the Γ valley, and A_n^{CL} and E_n^{CL} are the Γ to L intervalley phonon absorption and emission rates for the n th level in the Γ valley. These rates are calculated using Eqs. (2.10) and (2.30) of Ref. 6 with the material parameters of Ref. 4 and a deformation potential⁷ of 10^9 eV/cm. C_n^0 is the degeneracy of the n th level of the Γ valley and is given by

$$C_n^0 = 3.87 \times 10^{18} (1 + 1.24 E_n) \times [E_n (1 + 0.62 E_n)]^{1/2} \text{ cm}^{-3} \quad 1 \leq n \leq 18 \quad (2)$$

from Eqs. (76) and (77) of Ref. 4. The rate equations for L_n are analogous to Eq. (1), except that there are no levels below $n = 9$. Similarly, the degeneracy of the n th level, L_n^0 is given by

$$L_n^0 = 1.03 \times 10^{20} [1 + 0.92 (E_n - 0.29)] \times \{(E_n - 0.29) [1 + 0.46 (E_n - 0.29)]\}^{1/2} \quad 9 \leq n \leq 18, \quad (3)$$

where $E_n = (n - 0.5) \times 0.036$ eV. The initial photoexcited carrier population is placed in the $n = 14$ level in the central valley or L valley. The time evolution of C_5 gives the calculated time dependence of the split-off transition.

Equation (1) and the corresponding equations for L_n were integrated numerically for the range of photoexcited carrier densities of 0.1 – 2.0×10^{19} cm^{-3} and for a range of phonon temperatures from $T_p = 300$ – 1800 K. The experimentally observed threshold behavior of wing height versus n_e was most closely reproduced in these simulations with $T_p = 300$ – 450 K. (For definiteness, we use $T_p = 300$ K in the results presented here.) This implied rapid cooling of the electron distribution is not surprising since our samples are at room temperature.

In Fig. 3 the evolution in time of C_5 is shown. The rise times of these curves vary from 1.8 to 0.7 ps, depending on n_e . These results are in reasonable agreement with the GaAs data with a range of approximate rise times of 1.7 – 1.3 ± 0.2 ps for densities of 0.5 – 2.0×10^{19} cm^{-3} , as well as with our MQW data with a 1.0 ± 0.2 ps rise time at a carrier density of 2×10^{19} cm^{-3} . The GaAs and MQW data are similar because in the MQW there is no excitation in the AlGaAs barrier layer as a result of the high concentration of Al.

The calculated final electron population C_5 is proportional to the height of the rising wing. A comparison of the

calculated and the measured wing height versus n_e reveals good qualitative agreement. In both cases, there is a threshold density n_{th} below which no rising wing is observed, and there is a linear increase in the rising wing height with n_e for a range of n_e up to five times larger than n_{th} . Since our experimental signal is an average over a range of densities due to the finite thickness of the sample, exact agreement between theory and experiment is not expected, especially in the amplitude of the signal.

A similar numerical simulation was performed for AlGaAs in the same photoexcited density range. When looking at the population of the light and heavy hole transition regions (since there is no split-off band transition) no rising wing was seen, only the decay of the initial population.

In conclusion, we have observed the dynamic Burstein–Moss shift following intense photoexcitation at 0.5 eV in GaAs and MQW structures. We have measured a characteristic band-filling time of 1.7–1.3 ps in GaAs for $n_e = 0.5$ – 2.0×10^{19} cm^{-3} and 1 ps in a MQW structure for $n_e = 2 \times 10^{19}$ cm^{-3} . These band-filling times correspond to the redistribution of electrons from an initially excited energy of 0.5 eV above the bottom of the conduction band to the split-off band transition at an energy of 0.15 eV. An approximate rate equation model, which considers only unscreened electron-phonon scattering and assumes a constant phonon temperature near the lattice temperature corresponding to a rapid cooling of phonons, agrees reasonably well with the experimental results. The question of screening in the presence of a nonequilibrium carrier distribution needs further consideration.

We thank Dr. Vilnis Kreismanis for sample growth and preparation. This work was supported by the NSF through the Materials Science Center of Cornell University and by the Joint Services Electronics Program.

¹E. Burstein, Phys. Rev. **93**, 632 (1954); T. S. Moss, Proc. Phys. Soc. (London) B **76**, 775 (1954).

²D. J. Erskine, A. J. Taylor, and C. L. Tang, Appl. Phys. Lett. **45**, 54 (1984); A. J. Taylor, D. J. Erskine, and C. L. Tang, Appl. Phys. Lett. **43**, 989 (1983); Chem. Phys. Lett. **103**, 430 (1984).

³C. V. Shank and D. H. Auston, Phys. Rev. Lett. **34**, 479 (1975); C. V. Shank, R. L. Fork, R. F. Leheny, and Jagdeep Shah, Phys. Rev. Lett. **42**, 112 (1979).

⁴J. S. Blakemore, J. Appl. Phys. **53**, R123 (1982).

⁵B. P. Zakharchenya, D. N. Mirlin, V. I. Perel', and I. I. Reshine, Sov. Phys. Usp. **25**, 143 (1982).

⁶W. Fawcett, A. Boardman, and S. Swain, J. Phys. Chem. Solids **31**, 1963 (1970).

⁷M. A. Littlejohn, J. Hauser, and T. Glisson, J. Appl. Phys. **48**, 4587 (1977).